

# Electrochemical Preparation of Platinum Nanocrystallites on Activated Carbon Studied by X-ray Absorption Spectroscopy

Sébastien Adora,\* Yvonne Soldo-Olivier, René Faure, and Robert Durand

Laboratoire d'Electrochimie et de Physico-chimie des Matériaux et des Interfaces (INPG/CNRS) ENSEEG, BP 75, 38402 Saint Martin D'Hères, France

Elizabeth Dartyge and François Baudalet

Laboratoire pour l'Utilisation du Rayonnement Electromagnétique, Centre Universitaire Paris—Sud, 91405 Orsay, France

Received: December 18, 2000

An XAS investigation was undertaken to understand the mechanism of our platinum deposition process. This process is based on  $\text{H}_2\text{PtCl}_6$  impregnation onto activated carbon followed by current pulses reduction. After each step of the process and during the electrochemical reduction, ex situ and in situ dispersive X-ray absorption measurements allowed us to follow the evolution of platinum environment and its valence state. This characterization shows a first diminution in the electronic density of final states for Pt atoms when  $\text{H}_2\text{PtCl}_6$  is involved in the impregnation mixture, because of the simple contact of this acid with activated carbon. After the impregnation mixture spraying step onto a carbon support and thermal treatment, the platinum compound is found to be reduced to a Pt(II) form corresponding to the anionic  $\text{PtCl}_4^{2-}$  complex. The electrochemical reduction takes place in the first galvanostatic pulses. The competitive proton evolution to hydrogen on in situ generated metallic platinum particles occurs, but EXAFS analysis shows that, in our process, this evolved hydrogen does not have a major role in platinum species reduction.

## 1. Introduction

Platinum nanoparticles synthesis is of great interest for catalysis and electrocatalysis applications<sup>1–4</sup> (hydrogen or methanol oxidation and oxygen reduction in fuel cells, hydrocarbon conversion, and so on). Catalytic properties are sensitive to the particles' shape and size and to the nature of the support.

Several methods of preparation have been used. Zoval et al.<sup>1</sup> listed (1) the colloid based method, (2) the metal evaporation, (3) the reduction of metal salt particles adsorbed on a support with  $\text{H}_2$  in gas phase, and (4) the electrochemical reduction of platinum salt in solution. Reduction by  $\text{H}_2$  at room temperature<sup>2</sup> and the use of a reducing agent ( $\text{Na}_2\text{S}_2\text{O}_4$ ) in solution<sup>5</sup> or hydrogen donor<sup>6</sup> have also been tried.

In this paper, we report on a method based on hexachloroplatinic acid impregnation on carbon followed by an electrochemical reduction step composed of several current pulses.<sup>7,8</sup> The aim is the preparation of platinum nanoparticles in the range of 2–5 nm with high  $w_{\text{Pt}} = m_{\text{Pt}}/(m_{\text{Pt}} + m_{\text{C}})$  mass ratios that are required for fuel cell electrodes. Carbon support is used because of its absence of catalytic activity and for its good electronic conductivity properties allowing the electrochemical preparation of metallic nanoparticles.<sup>1</sup>

However, an important question to be answered deals with the platinum species adsorption process on the carbon surface. Shimazu et al.<sup>9</sup> observed that a glassy carbon electrode simply immersed in  $\text{H}_2\text{PtCl}_6$  solution gives a current for hydrogen

evolution after a water rinse; scanning electron microscopy (SEM) observation revealed platinum particles. They think that these particles are probably formed during the cathodic scan of the voltammetry, a technique used to measure the electrode activity. Zoval et al.<sup>1</sup> worked on highly oriented pyrolytic graphite (HOPG). By ex situ atomic force microscopy (AFM) observations, they pointed out a spontaneous reduction of  $\text{H}_2\text{PtCl}_6$ , giving rise to particles 2–2.5 nm in diameter on the HOPG plane edges and even on its basal planes. After selected area electron diffraction (SAED) analysis, they concluded that the particles correspond to metallic platinum. The explanation proposed for this platinum reduction phenomenon is simultaneously based on the oxidation of incompletely oxidized surface functional groups and on the conduction properties of isolated delaminated graphitic islands.

On the other hand, ex situ X-ray photoelectron spectroscopy (XPS) measurements performed on impregnated activated carbon dried in a vacuum by van Dam et al.<sup>10</sup> report the presence of Pt(II) and Pt(IV) compounds on the carbon surface.

With high-resolution angle resolved XPS (ARXPS) experiments on the platinum compound (Pt(II)) adsorbed on oxidized carbon fibers, Yue et al.<sup>11</sup> assign the different platinum peaks to Pt(IV), Pt(II), and Pt(0).

De Miguel et al.<sup>12</sup> give more detailed chemical information about the impregnation step of platinum on carbon by Extended X-ray absorption fine structure (EXAFS) data analysis. Changes in the amplitude of the Fourier transformed Pt–Cl peak are observed between the spectra of  $\text{H}_2\text{PtCl}_6$  and of the sample after the impregnation and drying steps; furthermore, platinum–platinum peaks are not present in their Fourier transformed spectra. The authors explain their results using the model

\* To whom correspondence should be addressed. Laboratoire d'Electrochimie et de Physico-chimie des Matériaux et des Interfaces (INPG/CNRS) ENSEEG, 1130 Rue de la Piscine, Domaine universitaire BP 75, 38402 Saint Martin D'Hères, France. E-mail: Sebastien.Adora@enseeg.inpg.fr. Fax: (+ 33) 4 76 82 67 77. Phone: (+33) 4 76 82 65 88.

proposed by van Dam et al.,<sup>10</sup> i.e., in terms of four chlorine atoms surrounding each platinum atom (or fewer than four but with an anchorage on a carbon or oxygen atom). To further elucidate the nature of this platinum complex (neutral  $\text{PtCl}_4$ <sup>13</sup> or the anionic form<sup>14</sup>) and its link with the carbon surface, detailed EXAFS spectra modeling is required.

The anchorage(s) of the platinum complex and the platinum particle is (are) still unknown. Prado-Burguette et al.<sup>15</sup> propose the formation of a Pt–O complex on the surface, whereas Lampitt et al.<sup>2</sup> fit their EXAFS spectra with two Pt–C distances. These distances of 2.6 and 3.6 Å are based on the epitaxial growth of platinum particles on the basal (0001) plane of carbon. However, as pointed out by Sepúlveda-Escribano et al.,<sup>16</sup> conflicting results are reported in the literature on this subject.

This paper is devoted to the analysis by X-ray absorption spectroscopy (XAS) of the successive steps of our platinum particles preparation process.<sup>7,8</sup> XAS has already provided a lot of information in catalysis,<sup>17</sup> electrocatalysis (in situ characterization<sup>2,18–21</sup>), and carbon supported catalyst synthesis.<sup>22,23</sup> As the sample characterization must be done after each current pulse in less than one minute, the dispersive XAS technique was chosen.

## 2. Experimental Section

**2.1. Electrode Preparation.** Our impregnation mixture is based on four compounds.

(1) Activated carbon: Vulcan XC72R (Cabot) was treated under  $\text{CO}_2$  at 980 °C in order to decrease the amount of surface impurities and to open the microporosity, and then quenched at room temperature after treatment to set the oxygen functional surface groups.

(2) Solvents: ultrapure water (Millipore system, resistivity > 18 MΩ cm) and ethanol (95–96% in volume, Prolabo R. P. Normapur) or 2-propanol (99.7% in volume, Prolabo R. P. Normapur) were used to improve the carbon wettability.

(3) A Nafion solution was used in order to achieve a mass ratio carbon/Nafion of one (Nafion solution 5% in mass in a mixture of lower aliphatic alcohols and water, from Aldrich). This ratio allows us to have carbon percolation (hence, electronic conduction) and the mechanical stability of the layer.

(4) Hexachloroplatinic acid, from Prolabo R. P. Normapur, was used.

The platinum acid powder is dissolved in water in order to get a 0.1 mol L<sup>−1</sup> solution. The amount of solution corresponding to the desired  $w_{\text{Pt}} = m_{\text{Pt}}/(m_{\text{Pt}} + m_{\text{C}})$  mass ratio is mixed with activated carbon and solvents (1 volume of alcohol for 5 of water). When adsorption equilibrium is achieved, Nafion is added to form the complete impregnation mixture. This mixture is sprayed on a carbon support (Toray Carbon Paper, TGPH-120 Plain E-Tek) to obtain the required platinum loading: 0.1 mg cm<sup>−2</sup> for real fuel cell electrodes but 0.5–1 mg cm<sup>−2</sup> for transmission XAS experiments, for which such high loading is necessary to improve the platinum XAS signal/noise ratio for in situ experiments. The solvents are evaporated on a hotplate between 120 and 150 °C, and then a further thermal treatment is done in order to strengthen the carbon–Nafion structure (150 °C for 10 min). A disk of 0.8 cm in diameter is then cut to be used as the working electrode in our electrochemical cell (see below section 2.3.2.).

**2.2. Electrochemical Reduction.** The reduction is based on current pulses (the only industrial realistic process).<sup>7</sup> The first pulse (prepulse) corresponds to a charge of  $-0.2 \text{ C cm}^{-2}$  for a duration of 0.2 s. Then a series of pulses, longer in time (typically 1 s) but with a similar coulometry, are applied. Because of competitive hydrogen formation during the pulses, the total

applied coulometry is twice the strict minimum needed to reduce completely all of the platinum species<sup>35</sup> assuming an initial Pt valence state of 4. Successive pulses are separated by a 1 min time interval. Application of the pulse train was realized with a computer-controlled EG&G 273A potentiostat/galvanostat, using the M270 EG&G program.

**2.3. X-ray Absorption Spectroscopy Experiments.** **2.3.1. XAS Parameters.** X-ray absorption measurements at the Pt–L<sub>III</sub> edge were carried out at the D11 beam line (dispersive XAS) of the Laboratoire pour l'Utilisation du Rayonnement Electromagnétique (LURE, Orsay), using synchrotron radiation of the DCI positron storage ring (1.85 GeV).

A dispersive bent triangular shaped crystal (Si 111) was used to focus onto the sample the polychromatic X-ray beam ( $10^{10}$  photons s<sup>−1</sup>). Then the beam diverged toward a position sensitive detector made of 1024 sensing elements (2500 μm in high, 25 μm wide). The sample (solution, electrode, or electrode in the electrochemical cell) was aligned so that the focused X-ray beam, with an area of 0.2 cm<sup>2</sup>, passed through it.

One spectrum recording, which was already the average of 16 measurements, lasted less than 1 s. The number of recordings accumulated to achieve the final spectrum was a function of the amount of platinum in the sample and of the sample absorption. A total of 10 recordings revealed enough to follow the evolution of the different bond contributions around the absorbing platinum atom (Pt–Cl, Pt–Pt, etc.) in the EXAFS spectrum during the electrochemical reduction.

In the transmission mode, the absorption is defined by  $\ln(I_0/I)$ , where  $I_0$  and  $I$  are the incident and transmitted signals, respectively. In our dispersive XAS experiment, the presence of one absorbing detector made it necessary to realize two different experiments, without and with the absorber element, to acquire the data necessary to extract the absorption spectra. So, for each electrode placed in or out of the electrochemical cell, a sample identical to the real electrode, but without platinum, was used to record  $I_0$ . These  $I_0$  recordings allowed us to take into account the noncompletely negligible and energy-dependent absorption by carbon, polyethylene, etc. (see below the component of the electrochemical cell).

**2.3.2. XAS Electrochemical Cell.** For XAS in situ electrochemical measurements, a particular cell with a compromise between electrochemistry and XAS requirements was used (Figure 1a). The cell body consisted of two polyethylene plates. The central part of each was as thin as possible (less than 0.2 mm) to reduce beam absorption. The working electrode (0.5 mg cm<sup>−2</sup> Pt loading, geometric area: 0.50 cm<sup>2</sup>), the electrolyte (Nafion membrane), and the counter electrode (plate of Toray Carbon Paper) were pressed between these plates. Electrical connections were achieved by laminated gold wires. To reach a 1 mg cm<sup>−2</sup> Pt loading useful for XAS experiments, in some cases, two identical electrodes situated in front of each side of the counter electrode were connected in parallel, providing two cells in series on the beam.

This cell was set in a glass beaker (Figure 1b) containing at the bottom a 0.5 mol L<sup>−1</sup> sulfuric acid electrolyte (sulfuric acid 96% Suprapur from Merck), in which a narrow strap of the Nafion membrane and the tip of the reference electrode capillary were immersed. A polytetrafluoroethylen (PTFE) cover with five entries allowed solution and cell deaeration by a nitrogen flux, electrical connections, and alignment of the cell. The X-ray beam crossed the glass beaker through two holes with Kapton windows, which prevented air inlet.

**2.3.3. XAS Data Analysis.** First of all, collected absorption data are function of the sensing element in the detector and

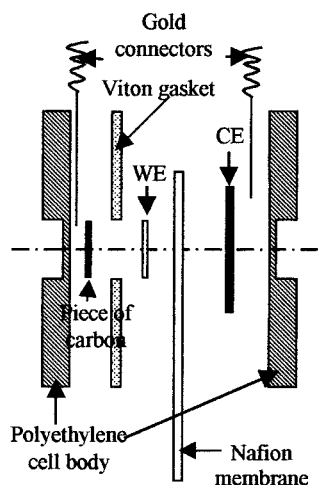


Figure 1a

**Figure 1.** Specific electrochemical cell for in situ X-ray absorption spectroscopy (1a) and glass cell allowing to work with deaerated electrolyte (1b). WE, working electrode; CE, counter electrode.

**TABLE 1: Values for Pt–Pt, Pt–O, Pt–Cl, and Pt–C Interatomic Distances Found in Literature for Different Compounds**

bond	distance	ref
Pt–Pt (bulk)	2.77 Å	2, 18
Pt–Pt nanoparticles	2.64–2.77 Å	28
Pt–O (Na <sub>2</sub> Pt(OH) <sub>6</sub> )	2.05 Å	2
Pt–O (Pt(CH <sub>3</sub> COO) <sub>2</sub> ) <sub>4</sub>	2.00 and 2.16 Å	23
Pt–O in PtO <sub>2</sub>	2.07 Å	18
Pt–O nanoparticles	2.03–2.07 Å	18, 29
Pt–Cl in K <sub>2</sub> PtCl <sub>6</sub>	2.32 Å	30
Pt–Cl in K <sub>2</sub> PtCl <sub>4</sub>	2.33 Å	13
Pt–Cl in PtCl <sub>4</sub>	2.26 Å	14
Pt–C in Rb <sub>2</sub> Pt(CN) <sub>4</sub>	1.99 Å	31
Pt–C (“epitaxy” onto carbon basal plane)	2.5–2.62 Å (nearest C atoms)	2
	3.3–3.6 Å (second C atoms)	2
Pt–C (in organometallic compounds with benzene ligand)	2.2 Å	2

must be plotted vs the incident photon energy ( $E$ ). This conversion requires acquisition of data on a reference before each experiment, as well as a knowledge of its absorption  $\mu = f(E)$  relation. This pixel-energy conversion was performed with data from a Pt foil reference at the Pt–L<sub>III</sub> absorption edge using the Miguel’s program CDXAS 2.6.<sup>24</sup>

The principles of EXAFS spectra extraction and simulation are described elsewhere.<sup>25</sup> The analysis was performed using the SEDEM software<sup>26</sup> written by Aberdam.

After a classical background removal, the EXAFS signals  $\chi(k)$  were obtained, and in order to minimize truncation effects, a Kaiser Plateau window with parameter  $\tau = 2.5$  was applied to the  $k$  weighted  $\chi(k)$  function prior to Fourier transforming. In real space, the first principal hump was isolated. EXAFS oscillations modeling was achieved on the inverse Fourier transformation of this distance(s) contribution(s). For each shell, the parameters of the modeling are the coordination number ( $N$ ), the interatomic distance ( $r$ ), the Debye–Waller factor ( $\sigma^2$ ), and the energy shift ( $\Delta E_0$ ). Modeling was performed by

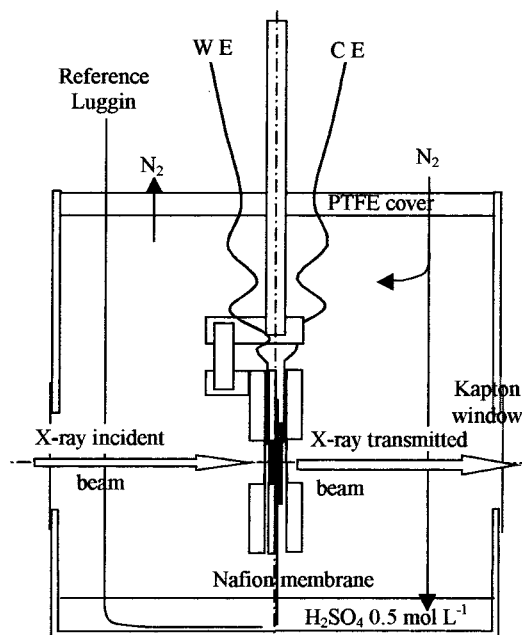


Figure 1b

combination of various kinds of bond (in our case, chlorine, platinum, oxygen, and carbon atoms could be linked with platinum absorbing atom).

To describe the Pt–Pt, the Pt–Cl, and the Pt–O bond, the reference samples used as a model from which backscattering amplitude and phase shift files have been extracted are metallic Pt, K<sub>2</sub>PtCl<sub>6</sub> (99.99% from Aldrich), and PtO<sub>2</sub> (99.95% PtO<sub>2</sub> from Johnson Matthey), respectively. Theoretical Pt–C phase and amplitude have been calculated using FEFF6.01<sup>27</sup> on the reference compound K<sub>2</sub>Pt(CN)<sub>4</sub> (four carbon atoms at a distance of 1.99 Å from the absorbing Pt).

The prefactor  $S_0^2$  was fixed at 0.9.

References used in previous literature experiments<sup>2,13,14,18,23,28–31</sup> are reported in Table 1.

**2.4. Particle Size Characterization.** Platinum particle sizes were measured by ex situ transmission electron microscopy (TEM) observations (JEOL 200CX).

### 3. Results and Discussion

**3.1. From H<sub>2</sub>PtCl<sub>6</sub> to Impregnation Mixture.** At the beginning of the process, water is added to hexachloroplatinic acid (H<sub>2</sub>PtCl<sub>6</sub>) leading to a 0.1 mol L<sup>−1</sup> solution. Then the impregnation mixture is prepared. As described in the Experimental Section, it is a mixture of alcohol, water, activated carbon, the previous solution, and Nafion.

To determine the effects of the different compounds and their interactions, several partial mixtures—H<sub>2</sub>PtCl<sub>6</sub> solution, H<sub>2</sub>PtCl<sub>6</sub> solution plus alcohol (here 2-propanol), and H<sub>2</sub>PtCl<sub>6</sub> solution plus activated carbon—have been characterized and compared to the complete mixture.

As shown on Table 2 (parts 1, 4, and 5), the relative height of the white line falls from 2.2 for H<sub>2</sub>PtCl<sub>6</sub> 0.1 mol L<sup>−1</sup> solution down to about 1.6 for the complete impregnation mixtures. This decrease in the electronic density of the final states above the Fermi level for platinum is independent of the  $w_{Pt}$  mass ratio and of the nature of the alcohol (Table 3 parts 1, 3, and 5).

2-Propanol alone does not modify, at least in the short term, the electronic state of Pt (experiments were carried at room

**TABLE 2: Transformation Ranges for the Forward ( $\Delta k$ ) and Inverse ( $\Delta r$ ) Fourier Transforms and Structural Parameters for the Pt–Cl Bond Obtained from the Analysis of EXAFS Spectra at the Pt–L<sub>III</sub> Edge for (1) a H<sub>2</sub>PtCl<sub>6</sub> 0.1 mol L<sup>−1</sup> Aqueous Solution; This Same Solution with Respectively (2) Isopropanol or (3) Carbon ( $w_{\text{Pt}} = 12\%$ ); (4) a  $w_{\text{Pt}} = 20\%$  Complete Impregnation Mixture with Isopropanol; and (5) a  $w_{\text{Pt}} = 30\%$  Complete Impregnation Mixture with Ethanol**

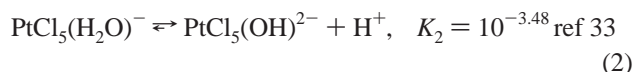
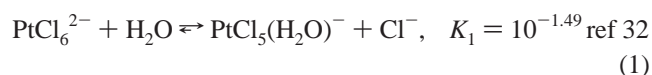
	white line height (a.u.)	$\Delta k/\text{\AA}^{-1}$	$\Delta r/\text{\AA}$	chlorine shell			
				$N$	$r/\text{\AA}$	$\sigma^2/\text{\AA}^2$	$\Delta E_0/\text{eV}$
(1) H <sub>2</sub> PtCl <sub>6</sub>	2.2	3.3–11.4	1.00–2.48	5.6 (imposed)	2.32 ( $\pm 0.01$ )	$4.8 \times 10^{-3}$ ( $\pm 3 \times 10^{-3}$ )	−1.0 ( $\pm 0.4$ )
(2) H <sub>2</sub> PtCl <sub>6</sub> with 2-propanol	2.2	3.2–11.0	1.34–2.44	5.2 ( $\pm 0.3$ )	2.31 ( $\pm 0.01$ )	$4.8 \times 10^{-3}$ ( $\pm 3.0 \times 10^{-3}$ )	−1.3 ( $\pm 1.4$ )
(3) H <sub>2</sub> PtCl <sub>6</sub> with activated carbon	1.9	3.2–10.8	1.14–2.44	5.5 ( $\pm 0.5$ )	2.30 ( $\pm 0.01$ )	$5.2 \times 10^{-3}$ ( $\pm 3.3 \times 10^{-3}$ )	−1.9 ( $\pm 1.0$ )
(4) Impregnation mixture $w_{\text{Pt}} = 20\%$ with 2-propanol	1.62	3.2–10.8	1.14–2.44	5.0 ( $\pm 0.4$ )	2.33 ( $\pm 0.01$ )	$5.7 \times 10^{-3}$ ( $\pm 0.5 \times 10^{-3}$ )	−0.7 ( $\pm 0.9$ )
(5) Impregnation mixture $w_{\text{Pt}} = 30\%$ with ethanol	1.64	3.2–11.4	1.14–2.54	5.4 ( $\pm 0.3$ )	2.32 ( $\pm 0.01$ )	$6.1 \times 10^{-3}$ ( $\pm 0.7 \times 10^{-3}$ )	−0.8 ( $\pm 0.8$ )

**TABLE 3: Fourier Transformation Ranges for the Forward ( $\Delta k$ ) and Inverse ( $\Delta r$ ) Fourier Transforms and Structural Parameters for the Pt–Cl Bond Obtained from the Analysis of EXAFS Spectra at the Pt–L<sub>III</sub> Edge for Impregnation Mixtures with Mass Ratios  $w_{\text{Pt}} = 20\%$  or  $30\%$  with Ethanol or 2-Propanol and for Electrodes Prepared from These Mixtures after Spray and Heat Treatment but before Any Electrochemical Reduction**

	white line height (a.u.)	$\Delta k/\text{\AA}^{-1}$	$\Delta r/\text{\AA}$	chlorine shell			
				$N$	$r/\text{\AA}$	$\sigma^2/\text{\AA}^2$	$\Delta E_0/\text{eV}$
(1) Impregnation mixture $w_{\text{Pt}} = 20\%$ with ethanol	1.69	3.1–11.3	1.14–2.44	5.2 ( $\pm 0.2$ )	2.32 ( $\pm 0.01$ )	$4.9 \times 10^{-3}$ ( $\pm 0.5 \times 10^{-3}$ )	−1.5 ( $\pm 0.5$ )
(2) Electrode from this 20% mixture with ethanol	1.22	3.0–10.9	1.16–2.44	3.6 ( $\pm 0.3$ )	2.32 ( $\pm 0.01$ )	$7.4 \times 10^{-3}$ ( $\pm 1.2 \times 10^{-3}$ )	−2.5 ( $\pm 1.1$ )
(3) Impregnation mixture $w_{\text{Pt}} = 30\%$ with 2-propanol	1.55	3.1–10.9	1.14–2.44	5.0 ( $\pm 0.6$ )	2.32 ( $\pm 0.01$ )	$5.2 \times 10^{-3}$ ( $\pm 3.3 \times 10^{-3}$ )	−1.3 ( $\pm 1.5$ )
(4) Electrode from this 30% mixture with 2-propanol	1.33	3.0–12.2	1.10–2.44	3.7 ( $\pm 0.4$ )	2.31 ( $\pm 0.01$ )	$4.6 \times 10^{-3}$ ( $\pm 1.0 \times 10^{-3}$ )	−3.1 ( $\pm 1.1$ )
(5) Impregnation mixture $w_{\text{Pt}} = 30\%$ with ethanol	1.64	3.2–11.4	1.14–2.54	5.4 ( $\pm 0.3$ )	2.32 ( $\pm 0.01$ )	$6.1 \times 10^{-3}$ ( $\pm 0.7 \times 10^{-3}$ )	−0.8 ( $\pm 0.8$ )
(6) Electrode from this 30% mixture with ethanol	1.22	3.2–10.8	1.16–2.46	3.9 ( $\pm 0.3$ )	2.31 ( $\pm 0.01$ )	$5.7 \times 10^{-3}$ ( $\pm 1.1 \times 10^{-3}$ )	−3.5 ( $\pm 0.4$ )

temperature with a laps of time between preparation and characterization not exceeding one week), whereas the white line variation shows that platinum acid interacts with carbon even in absence of alcohol (see Table 2 parts 1–3). The greater diminution of the near edge region intensity with both active carbon and 2-propanol might be explained by a better carbon wettability in the presence of alcohol (larger number of adsorption sites available) than with water alone.

EXAFS modeling does not show any significant evolution in the local structure. The Pt–Cl inter atomic distance  $r$  remains constant at around 2.32 Å for the studied compounds (partial and impregnation mixtures) and, within the error bars, the number  $N$  of chlorine atoms nearest neighbors does not vary. The number of chlorine atoms found (fewer than six) agrees with the constants given in the literature for the different acid/base and complex couples.<sup>32,33</sup> Considering that H<sub>2</sub>PtCl<sub>6</sub> is a strong acid<sup>33</sup> and that the reaction 1 is the preponderant one, the calculated number of Pt–Cl bonds for a 0.1 mol L<sup>−1</sup> H<sub>2</sub>PtCl<sub>6</sub> solution, for a 20% and a 30%  $w_{\text{Pt}}$  impregnation mixtures are 5.6, 5.3, and 5.4, respectively. As seen from Table 2, we have a good agreement between theoretical and experimental results:



To achieve six bonds around the platinum atom, the carbon and/or oxygen shell must be introduced in our EXAFS simulation.

Nevertheless, this introduction does not improve the quality of the fit. As an example, Figure 2 shows the Fourier filtered contribution of the first peak (experimental and simulated curves) for the H<sub>2</sub>PtCl<sub>6</sub> plus activated carbon mixture: the quality of the fit obtained considering only chlorine neighbors is satisfactory and is not improved by the addition of Pt–O and/or Pt–C bonds. So if O or C contributions are present, they are small, and within our signal/noise ratio, we are not able to detect them.

**3.2. Electrode Elaboration (Spray and Thermal Treatment).** Electrode manufacturing involves the evaporation of the solvents on a hotplate between 120 and 150 °C, followed by a 10 min reconstitution of the Nafion polymer at 150 °C.

Table 3 shows the first large transformation in the platinum environment. The white line height decreases from about 1.6 for the impregnation mixture to about 1.2 for the electrode, which indicates changes in the platinum chemical bonds; it is correlated to the fact that the number of chlorine atoms decreases to about four after the thermal treatment, and this effect is independent of the  $w_{\text{Pt}}$  ratio or the nature of the alcohol.

Several structures exist with four Pt–Cl bonds, particularly the neutral form PtCl<sub>4</sub> and the anionic one PtCl<sub>4</sub><sup>2−</sup>. Fortunately, the inter atomic distances between platinum and the first shell of chlorine atoms are very different in the two compounds. They are respectively 2.26 Å in PtCl<sub>4</sub><sup>13</sup> and 2.33 Å in K<sub>2</sub>PtCl<sub>4</sub><sup>14</sup> (Table 1). For all of the prepared electrodes, we find a Pt–Cl distance of about  $2.32 \pm 0.01$  Å, which leads us to exclude the presence of PtCl<sub>4</sub>. Furthermore, the EXAFS spectra of K<sub>2</sub>PtCl<sub>4</sub> (powder reference) and of our electrodes are very similar (Figure 3). We conclude that on our electrode the platinum complexes are



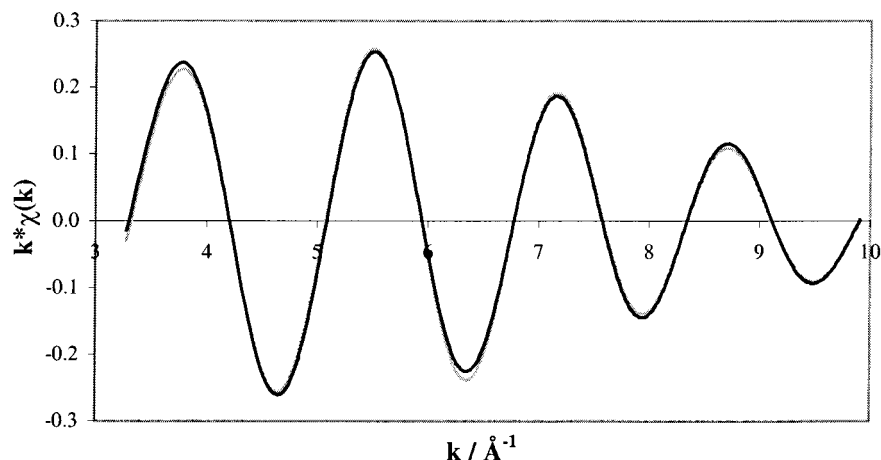


**Figure 2.**  $k$  weighted Fourier filtered EXAFS signal (in gray) and simulation (in black) of the impregnation mixture 20%  $w_{\text{Pt}}$  ethanol.

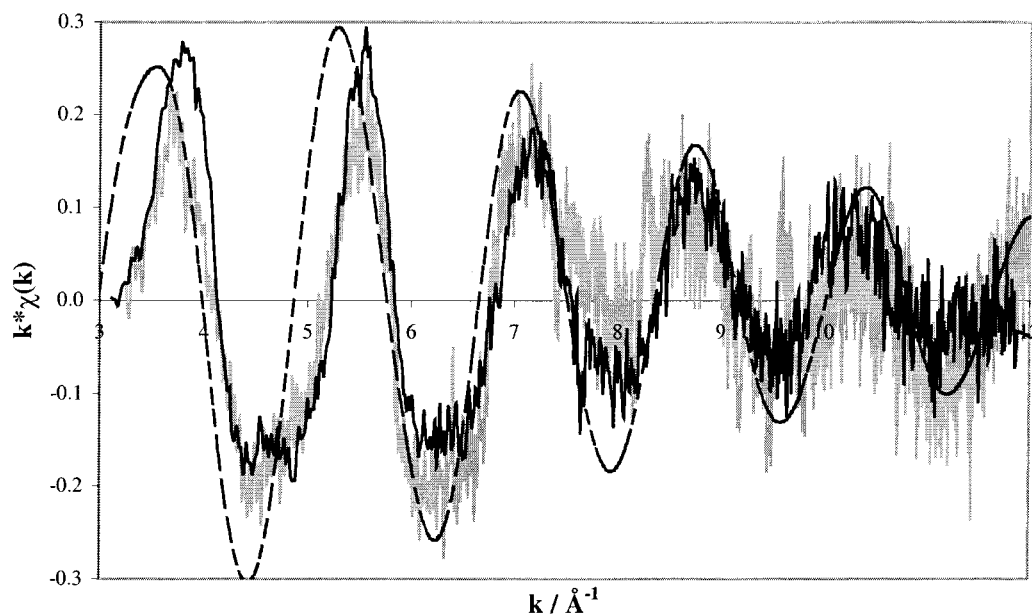


**Figure 3.**  $k$  weighted EXAFS experimental signals of (black line)  $\text{K}_2\text{PtCl}_4$  powder, (gray line) unreduced electrode based on a 30%  $w_{\text{Pt}}$  impregnation mixture with ethanol, and (dashed line) theoretical spectrum (generated with FEFF6.1a) of  $\text{PtCl}_4$ .

present in the form  $\text{PtCl}_4^{2-}$ , which is confirmed by the computation with FEFF 6.1a of the  $\text{PtCl}_4$  spectrum.

A thermal operation is often introduced<sup>1,10,12</sup> in electrode preparation. Even if the phenomena that occur during the different drying steps are difficult to control, particular attention must be paid on the possible prereduction of platinum species in this step. In fact, our experiments clearly show that when the impregnation mixture is sprayed and dried on the electrode a partial  $\text{H}_2\text{PtCl}_6$  reduction occurs, which terminates before the formation of metal particles.

As we have already commented in the previous paragraph, no other bond than Pt–Cl was used to correctly fit our spectra. If platinum bonds with carbon or with oxygen atoms of the surface functional groups are present, we cannot detect them.

Our results do not indicate a platinum complex adsorption on the carbon surface by numerous strong Pt–C or Pt–O bonds. Because the presence of  $\text{PtCl}_4^{2-}$  anions inside Nafion is very unlikely (Nafion is a cationic exchange membrane), we should consider weaker  $\text{PtCl}_4^{2-}$  adsorption on carbon, probably electrostatic-type adsorption on positively charged sites. These sites can be assigned to chromene or pyrone superficial functions.<sup>34</sup>

**3.3. Electrochemical Reduction.** The electrochemical description of our process will be published elsewhere,<sup>35</sup> and we

will focus here only on the information provided by in situ XAS experiments. The electrode was prepared from an impregnation mixture with a 30%  $w_{\text{Pt}}$  mass ratio and with ethanol as solvent.

The variation of the white line height for the initial electrode and for the electrode at different steps in the electrochemical process is negligible.

The study of the EXAFS signals proved to be more interesting. After the prepulse, no Pt–Pt bonds appear, whereas the number of chlorine atoms decreases from  $3.9 \pm 0.3$  down to  $3.3 \pm 0.2$  (see Table 4). This result is disappointing. Perhaps the prepulse is too short (0.2 s) to allow, slower than expected,  $\text{PtCl}_4^{2-}$  surface diffusion and Pt atoms agglomeration to occur. If nuclei of metallic platinum are obtained with this prepulse, as it is the case in standard electrocrystallization from species in solution, they are too few to be detected.

The main part of the electrochemical reduction occurs between the first and the fifth pulse, corresponding to double the minimum number of coulombs needed to reduce all the Pt(II) species ( $\text{PtCl}_4^{2-}$ ) into Pt(0). We notice that the first pulse has a strong effect, whereas the prepulse has none. They have the same coulometry, but the pulse has a longer duration. As seen in Figure 4, the amplitude of the peak corresponding to the Pt–Cl bond decreases, whereas the amplitude of the hump

**TABLE 4: Transformation Ranges for the Forward ( $\Delta k$ ) and Inverse ( $\Delta r$ ) Fourier Transforms and Structural Parameters Obtained from the Analysis of EXAFS Spectra at the Pt–L<sub>III</sub> Edge for the Electrode Elaborated from the  $w_{\text{Pt}} = 30\%$  Impregnation Mixture with Ethanol Before and After Current Steps**

	$\Delta k/\text{\AA}^{-1}$	$\Delta r/\text{\AA}$	chlorine shell				platinum shell			
			$N$	$r/\text{\AA}$	$\sigma^2/\text{\AA}^2$	$\Delta E_0/\text{eV}$	$N$	$r/\text{\AA}$	$\sigma^2/\text{\AA}^2$	$\Delta E_0/\text{eV}$
electrode	3.2	1.16	3.9	2.31	$5.7 \times 10^{-3}$	−3.5				
	10.8	2.46	( $\pm 0.3$ )	( $\pm 0.01$ )	( $\pm 1.1 \times 10^{-3}$ )	( $\pm 0.4$ )				
prepulse	3.2	1.26	3.3	2.31	$5.7 \times 10^{-3}$	−3.5				
	11	2.52	( $\pm 0.2$ )	( $\pm 0.01$ )	(imposed)	(imposed)				
1st pulse	3.0	1.30	2.6	2.31	$5.7 \times 10^{-3}$	−3.5	2.8	2.78	$5.3 \times 10^{-3}$	5.3
	11.3	3.16	( $\pm 0.2$ )	( $\pm 0.01$ )	(imposed)	(imposed)	( $\pm 1.4$ )	( $\pm 0.02$ )	( $\pm 1.2$ )	( $\pm 3.2$ )
4th pulse	3.1	1.34	1.8	2.32	$5.7 \times 10^{-3}$	−3.5	5.0	2.79	$5.3 \times 10^{-3}$	5.4
	11.3	3.16	( $\pm 0.2$ )	( $\pm 0.01$ )	(imposed)	(imposed)	( $\pm 1.3$ )	( $\pm 0.02$ )	( $\pm 2.6 \times 10^{-3}$ )	( $\pm 1.7$ )
10th pulse	3.1	1.34	1.3	2.32	$5.7 \times 10^{-3}$	−3.5	5.7	2.77	$5.1 \times 10^{-3}$	2.6
	11.2	3.20	( $\pm 0.2$ )	( $\pm 0.01$ )	(imposed)	(imposed)	( $\pm 1.4$ )	( $\pm 0.02$ )	( $\pm 2.2 \times 10^{-3}$ )	( $\pm 1.9$ )
20th pulse	3.1	1.34	1.2	2.34	$5.7 \times 10^{-3}$	−3.5	6.3	2.77	$5.4 \times 10^{-3}$	3.5
	11.3	3.20	( $\pm 0.2$ )	( $\pm 0.01$ )	(imposed)	(imposed)	( $\pm 1.4$ )	( $\pm 0.02$ )	( $\pm 1.9 \times 10^{-3}$ )	( $\pm 0.9$ )

corresponding to the Pt–Pt distance increases. The data analysis allows us to quantify these variations (see Table 4). The number of platinum neighbors rises from 0 after the prepulse to  $6.3 \pm 1.4$  after 20 pulses, with an interatomic distance of about 2.77 Å (the same as for bulk metallic Pt). At the same time, the number of Pt–Cl bonds falls from  $3.3 \pm 0.2$  down to  $1.2 \pm 0.2$ . The error bars on the coordination number and the Debye–Waller factor for the platinum shell are important, because of the significant correlation between these two parameters.

TEM observations (Figure 5) show a homogeneous size distribution, in the range of 2–5 nm as diameter, for the particles obtained after the electrochemical reduction. From the literature,<sup>18,20,29</sup> the number of Pt–Pt bonds in metallic platinum particles should be between 9 and 11 for our diameter range (slightly depending on the applied electrode potential), whereas

we find a lower value. A possible explanation is that some platinum species was not reduced in our preparation. Because of the XAS requirements, we must work with layers about 10 times thicker than the ones used for real fuel cells.<sup>8</sup> It is possible that with these thicker layers we do not have sufficient electronic and/or ionic percolation both needed for the electrochemical reduction to occur. If platinum species are not completely reduced, the Pt–Cl bonds present after the electroreduction would not necessarily be due to Cl<sup>−</sup> adsorption on the surface of metallic platinum particles. We checked the rest potentials after the fifth and the following pulses: they are all more negative than −160 mV/ECS. At these potentials, it has been shown<sup>36</sup> that only a very small amount of chlorides are adsorbed on monocrystalline or polycrystalline Pt surfaces. For this reason, even if in the present case we have Pt nanoparticles with different facets and edges at the cluster surface, we deduce that a part of the Pt–Cl bonds are due to unreduced Pt species.

In conventional glass cells, hydrogen bubble formation is seen during the current pulses. It is obvious that there is a competition between electroreduction of platinum complexes to metal particles and hydrogen evolution on the electrodeposited platinum, explaining the need of more than the strictly necessary coulometry (i.e., −0.6 C) to transform all of the Pt(II) species into Pt(0). As expected, this competitive reaction, which is almost negligible for the prepulse, becomes the main reaction when a large part of the platinum has been reduced into metal, because the hydrogen evolution overvoltage is low on metallic platinum and, on the contrary, very high on carbon.

The question which electrochemistry cannot answer is related to the reducing effect of the evolved hydrogen on platinum species between two pulses. The platinum species complete reduction by molecular hydrogen at room temperature has already been observed: with Na<sub>6</sub>(Pt(SO<sub>3</sub>)<sub>4</sub>), a Pt(II) compound, in solution, it is a well-established phenomenon.<sup>2</sup>

Because of the large error bars on the platinum coordination numbers obtained from the EXAFS modeling on the two spectra acquired just after one pulse and 30 s later (Figure 6), we cannot make any conclusion on the possible reductive role of hydrogen, but the analysis shows that, if hydrogen produced during the pulse plays a role in the transformation of the unreduced platinum complexes, this role is weaker than the electrochemical one.

#### 4. Conclusions

XAS ex situ and in situ experiments allowed us to characterize the successive steps of a Pt/C catalyst preparation procedure. This study has pointed out the following conclusions:

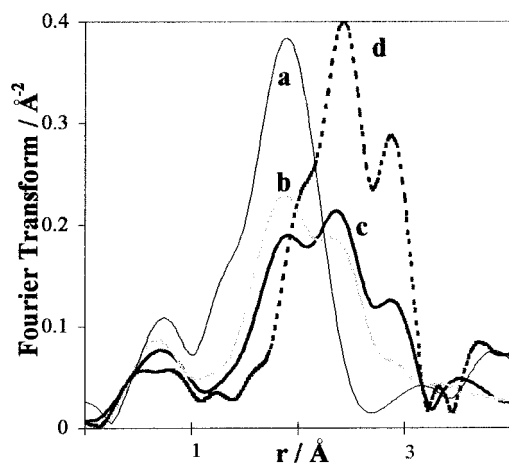


**Figure 4.** Fourier transform of  $k\chi(k)$  spectra: (a) unreduced electrode based on a 30%  $w_{\text{Pt}}$  impregnation mixture with ethanol; (b) and (c) after respectively 4 and 20 pulses; and (d) metallic platinum foil.

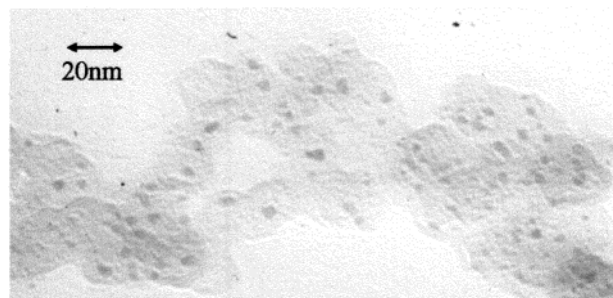


**Figure 5.** Transmission electron micrograph of electrochemically prepared platinum nanocrystallites on carbon ( $w_{\text{Pt}} = 20\%$ , 2-propanol, 0.12 mg cm<sup>−2</sup> Pt loading).

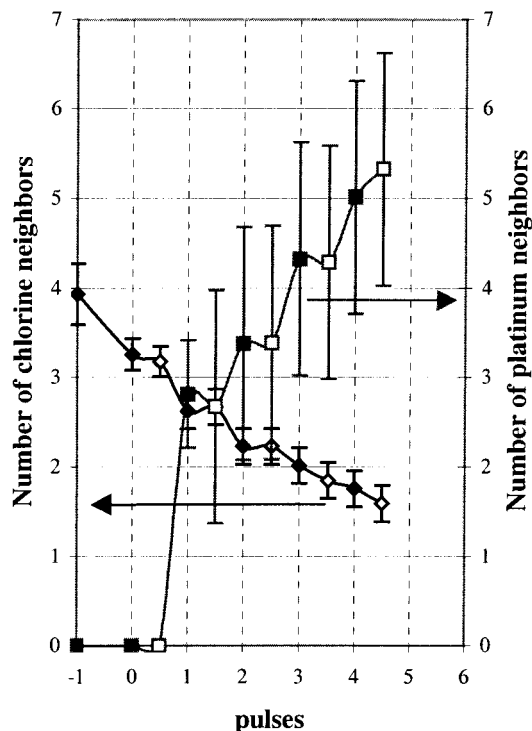


**Figure 6.** Evolution of the number of platinum nearest neighbors (chlorine  $\blacklozenge$  and platinum  $\blacksquare$  atoms) during the first steps of the electrochemical reduction. -1 means the unreduced electrode, and 0 and 0.5 mean the electrode just after the prepulse and 30 s after the prepulse. Two measurements have been done during each one minute time interval between successive pulses (full symbols: just after the pulse, empty symbols: 30 s after). Electrode parameters:  $w_{\text{Pt}} = 30\%$ ;  $0.5 \text{ mg cm}^{-2}$  Pt loading; ethanol.

(1) The white line intensity variations show a diminution in the electronic density of final states for Pt atoms when  $\text{H}_2\text{PtCl}_6$  forms an impregnation mixture with activated carbon and alcohol. In particular, a change is observed after the simple contact of the acid with the carbon. This modification is increased in the presence of a solvent (2-propanol or ethanol), probably because of a better carbon wettability.

The analysis of the EXAFS region does not reveal any significant variation in the local structure (no change in platinum environment). Furthermore, if Pt-O or Pt-C contributions to the signal are present, they are too small to be detected within our signal/noise ratio.

(2) A reduction of the platinum species to well-characterized  $\text{PtCl}_4^{2-}$  anions takes place when the impregnation mixture is sprayed onto a carbon support and heated. These Pt(II) anions are very probably adsorbed on the carbon surface, because they cannot be located inside the Nafion cationic membrane, but the presence of Pt-C and/or Pt-O bonds is difficult to detect.

(3) During the electroreduction process, the first short prepulse, conceived as a generator of nuclei, as in the classical electrocrystallization theory for nucleation growth from species in solution, does not seem to play a role. The main electrochemical reduction, resulting in metallic platinum nanoparticles, occurs in the first five pulses (corresponding to double the

numbers of coulombs necessary to reduce all initial Pt(II) species to Pt(0)). Simultaneous  $\text{H}_2$  evolution occurs, explaining the higher number of coulombs than theoretically expected for the reduction, but in our process, this evolved hydrogen does not play a major role in platinum reduction at room temperature.

## References and Notes

- (1) Zoval, J. V.; Lee, J.; Gorer, S.; Penner, R. M. *J. Phys. Chem. B* **1998**, *102*, 1166.
- (2) Lampitt, R. A.; Carrette, L. P. L.; Hogarth, M. P.; Russell, A. E. *J. Electroanal. Chem.* **1999**, *460*, 80.
- (3) Mansour, A. N.; Cook, J. W., Jr.; Sayers, D. E.; Emrich, R. J.; Katzer, J. R. *J. Catal.* **1984**, *89*, 462.
- (4) Savinova, E. R.; Simonov, P. A.; Cherstiouk, O. V.; Lebedeva, N. P.; Chuvilin, A. L. *51st Annual ISE meeting*; Warsaw, Poland, 2000, 161.
- (5) Antonucci, P. L.; Alderucci, V.; Giordano, N.; Cocke, D. L.; Kim, H. *J. Appl. Electrochem.* **1994**, *24*, 58.
- (6) Kinoshita, K. *Carbon, electrochemical and physicochemical properties*; Wiley: New York, 1988; Chapter 7, p 393.
- (7) Antoine, O.; Durand, R.; Gloaguen, F.; Novell-Cattin, F. European Patent No. 97400290, 1997.
- (8) Antoine, O. Ph.D. Thesis, INP, Grenoble, France, 1998.
- (9) Shimazu, K.; Weisshaar, D.; Kuwana, T. *J. Electroanal. Chem.* **1987**, *223*, 223.
- (10) van Dam, H. E.; van Bakkum, H. *J. Catal.* **1991**, *131*, 335.
- (11) Yue, Z. R.; Jiang, W.; Wang, L.; Toghiani, H.; Gardner, S. D.; Pittman, C. U., Jr. *Carbon* **1999**, *37*, 1607.
- (12) De Miguel, S. R.; Scelza, O. A.; Román-Martínez, M. C.; Salinas-Martínez de Lecea, C.; Cazorla-Amorós, D.; Linares-Solano, A. *Appl. Catal. A* **1998**, *170*, 93.
- (13) Wyckoff, R. W. G. *Crystal Structure*, 2nd ed.; Interscience Publishers: New York, 1964; Vol. 2, p 131.
- (14) Wyckoff, R. W. G. *Crystal Structure*, 2nd ed.; Interscience Publishers: New York, 1965; Vol. 3, p 69.
- (15) Prado-Burguete, C.; Linares-Solano, A.; Rodríguez-Reinoso, F.; Salinas-Martínez de Lecea, C. *J. Catal.* **1989**, *115*, 98.
- (16) Sepúlveda-Escribano, A.; Coloma, F.; Rodríguez-Reinoso, F. *Appl. Catal. A* **1998**, *173*, 247.
- (17) Iwasawa, Y. *J. Phys. IV France* **1997**, *7*, C2.
- (18) Herron, M. E.; Doyle, S. E.; Pizzini, S.; Roberts, K. J.; Robinson, J.; Hards, G.; Walsh, F. C. *J. Electroanal. Chem.* **1992**, *324*, 243.
- (19) Mukerjee, S.; Srinivasan, S.; Soriaga, M. P.; McBreen, J. *J. Electrochem. Soc.* **1995**, *142*, 1409.
- (20) Mukerjee, S.; McBreen, J. *J. Electroanal. Chem.* **1998**, *448*, 163.
- (21) Mukerjee, S.; McBreen, J. *J. Electrochem. Soc.* **1996**, *143*, 2285.
- (22) Pinxt, H. H. C. M.; Kuster, B. F. M.; Koningsberger, D. C.; Marin, G. B. *Catal. Today* **1998**, *39*, 351.
- (23) Román-Martínez, M. C.; Cazorla-Amorós, D.; Linares-Solano, A.; Salinas-Martínez de Lecea, C. *Curr. Top. Catal.* **1997**, *1*, 17.
- (24) San Miguel, A. *Physica B* **1995**, *177*, 208.
- (25) Koeningsberger, D. C.; Prins, R. *X-ray absorption: Principles, Applications, Techniques of EXAFS, SEXAFS and XANES*; Wiley: New York, 1988.
- (26) Aberdam, D. *J. Synchrotron Rad.* **1998**, *5*, 1287.
- (27) Rehr, J. J.; Mustre de Leon, J.; Zabinsky, S. I.; Albers, R. C. *J. Am. Chem. Soc.* **1991**, *113*, 5135.
- (28) Yoshitake, H.; Yamazaki, O.; Ota, K. I. *J. Electrochem. Soc.* **1994**, *141*, 2516.
- (29) Yoshitake, H.; Mochizuki, T.; Yamazaki, O.; Ota, K. I. *J. Electroanal. Chem.* **1993**, *361*, 229.
- (30) Shelimov, B.; Lambert, J. F.; Che, M. E.; Didillon, B. *J. Catal.* **1999**, *185*, 462.
- (31) O'Grady, W. E.; Koningsberger, D. C. Personal communication.
- (32) Davidson, C. M.; Jameson, R. F. *Trans. Faraday. Soc.* **1965**, *61*, 2462.
- (33) Shelimov, B.; Lambert, J. F.; Che, M.; Didillon, B. *J. Am. Chem. Soc.* **1999**, *121*, 545.
- (34) Donnet, J. B.; Voet, A. *Carbon Black—Physics, Chemistry, and Elastomer Reinforcement*; Marcel Dekker: New York, 1976; Chapter 4, p 144.
- (35) Antoine, O.; Srour, M.; Adora, S.; Durand, R. *J. New Mater. Electrochem. Syst.* Submitted for publication.
- (36) Li, N.; Lipkowski, J. *J. Electroanal. Chem.* **2000**, *491*, 95.